Available online at www.sciencedirect.com

ScienceDirect

Solar Energy 127 (2016) 96–108

SOLAR ENERGY

www.elsevier.com/locate/solener

A sensitivity analysis of the stepwise measurement procedure for the characterization of large area PV modules

Christoph Rapp *, Marc Steiner, Gerald Siefer, Andreas W. Bett

Fraunhofer Institute for Solar Energy Systems ISE, Heidenhofstr. 2, 79110 Freiburg, Germany

Received 21 September 2015; received in revised form 21 December 2015; accepted 22 December 2015

Communicated by: Associate Editor Takhir Razykov

Abstract

A major issue in the characterization of photovoltaic modules is the limitation of the homogenously irradiated area provided by the available sun simulators. Therefore the ***S**tepwise **M**easurement **P**rocedure for the Characterization of Large-area PV Modules* (*SMP*) was developed recently. This concept enables the characterization of modules with aperture areas larger than the area provided by a given sun simulator. In previous investigations the procedure demonstrated good applicability and high accuracy. In a real application environment, however, conditions like temperature and stray light might influence the measurement. Also, particular variations within a module like e.g. defective cells may lead to higher uncertainties for the results of the SMP. Therefore, an investigation of the impact of these factors on the accuracy of the procedure is performed. The results show that the impact of most factors can be minimized and even eliminated. Therefore, recommendations for the practical application are given.

Keywords: Characterization; Sun simulator; Electrical properties; Current voltage curve; PV modules; CPV modules

1. Introduction

The current–voltage (I–V) measurement of illuminated PV modules represent one of the most important characterization methods in photovoltaics. The most significant parameter extracted from the I–V curve is the **m**aximum **p**ower **p**oint (P_{MPP}). This quantity is needed to determine the efficiency of the module, and is the principal selling feature for PV modules. To determine the P_{MPP}, usually the modules are either illuminated with natural sunlight outdoors, or with sun simulators indoors. Indoor measurements have the principal advantage of being independent of daily, seasonally and weather dependent changes in the total and spectral irradiance as well as in the ambient temperature. The stable indoor conditions allow for short measurement times and a high reproducibility of the measurement. Over the past few years, the surface areas of PV and especially of **c**oncentrator PV (**CPV**) modules have constantly increased. This led to high investment and development costs for the enlargement of sun simulators. In the case of CPV, the discrepancy between the modules' surface areas (of up to 45 m^2 (Plesniak and Garboushian, 2011)) and the sun simulator's aperture area (largest for CPV applications: ~2.5 m^2 (Mathiak et al., 2014)) became so high that a comparable enlargement of the illuminated area is hardly possible. To solve this problem, the "**S**tepwise **M**easurement **P**rocedure (SMP) for the Characterization of Large-area PV Modules" has been introduced in Rapp et al. (2015). This procedure allows for the characterization of modules with aperture areas larger than the illuminated areas provided by sun simulators.

* Corresponding author.
E-mail address: christoph.rapp@ise.fraunhofer.de (C. Rapp).

http://dx.doi.org/10.1016/j.solener.2015.12.038
0038-092X/

The basic idea behind this procedure is a stepwise illumination of the full module area and simultaneous measurement of the resulting I–V curves – without the necessity of contacting the illuminated subunits of the module directly. With these I–V curves measured under partial illumination and the additionally measured dark I–V-curve, the I–V curve of the fully illuminated module can be calculated. In Rapp et al. (2015), the theoretical background of the procedure was derived and applied on modules with different cell interconnection schemes. The comparison of the I–V curves of the module under full illumination with the calculated I–V curves using the SMP, showed a very good agreement in the characteristic I–V parameters like I_{SC} and P_{MPP}. However, during the laboratory or industrial inline application of the procedure, conditions such as temperature and stray light might change. Also, the cells within a module can be of different production quality and may even include single defective cells. This could invalidate an assumption which was made in the derivation of the formula to calculate the module's I–V curve (Rapp et al., 2015, eq. 9) and thus lead to an error in the result of the SMP. To research the effect of these perturbing factors on the accuracy of the SMP, a sensitivity analysis concerning changes in temperature, stray light, and cells with non-ideal characteristics like high R_S and small R_P is presented. This analysis additionally shows what needs to be considered at the practical application of the procedure to minimize or even eliminate most of these aforementioned influences.

Firstly in this paper, a simulation model is introduced, which enables to simulate I–V curves of fully and partially illuminated CPV modules. This model is based on a temperature dependent SPICE (**S**imulation **P**rogram with **I**ntegrated **C**ircuit **E**mphasis, LTSpice, 2007) network model, which has been validated previously with measured data sets (Steiner et al., 2010, 2011). The I–V curves which are typically measured during the SMP (n partially illuminated and one dark I–V curve) can therefore be simulated. Using those curves, the I–V curve of the illuminated module can be calculated and compared with the simulated I–V curve under full illumination of the module. For modules with different cell interconnection schemes, a different manifestation of the individual effects under investigation is expected. Therefore, the study is performed on three different interconnection schemes, which cover a wide spectrum of possible cell interconnections.

2. Model description

2.1. General modeling approach to simulate CPV modules

Network simulations are a popular approach to simulate the I–V characteristics of multi-junction solar cells and modules (Steiner et al., 2011; Ota and Nishioka, 2012; Lv et al., 2015). The validated SPICE network model used in this work is described in Steiner et al. (2012) and is extended by the implementation of temperature dependent bypass diodes. The determination of the required cell parameters used in this model is explained in Steiner et al. (2010, 2011). In the following, the simulation of a lattice matched triple-junction (3J) solar cell including a bypass diode is illustrated. Through interconnection of many 3J cells, a suitable tool for the simulation of CPV modules with different interconnection schemes is given.

2.1.1. Simulation of a triple-junction cell

In Fig. 1, the electrical circuit of a 3J solar cell including a bypass diode is shown. In the model, the current density of each sub cell $J_i(V,T)$ is described by the two diode model, including a current source $J_{\mathrm{Ph},i}$ for the photo generated current density:

$$J_i(V,T) = J_{\mathrm{Ph},i} - J_{\mathrm{N},i} - J_{\mathrm{D},i}, \tag{1}$$

$$J_i(V,T) = J_{\mathrm{Ph},i} - J_{01,i}(T)\left[\exp\left[\frac{qV}{k_B T}\right] - 1\right] - J_{02,i}(T)\left[\exp\left[\frac{qV}{2k_B T}\right] - 1\right] \tag{2}$$

Here, the index i identifies the single sub cells: $i = 1$ top, $i = 2$ middle and $i = 3$ bottom. In Eq. (2), $J_{01,i}(T)$ is the dark saturation current density, which in combination with the exponential function describes the recombination current in the neutral region $J_{\mathrm{N},i}$. The dark saturation current density $J_{02,i}(T)$ in combination with the exponential function describes the recombination current in the depletion region $J_{\mathrm{D},i}$.

As the dark I–V curves for our purpose are simulated to be temperature dependent, the dark saturation current densities $J_{01,i}(T)$ and $J_{02,i}(T)$ are modeled as introduced by Reinhardt et al. (1995):

$$J_{01,i}(T) = k_{i1}T^3\exp\left[-\frac{E_{\mathrm{gap},i}(T) - \Delta E_{\mathrm{gap},i}}{k_B T}\right] \tag{3}$$

$$J_{02,i}(T) = k_{i2}T^{5/2}\exp\left[-\frac{E_{\mathrm{gap},i}(T) - \Delta E_{\mathrm{gap},i}}{2k_B T}\right] \tag{4}$$

The parameters k_{i1}, k_{i2} and $\Delta E_{\mathrm{gap},i}$ were taken from Steiner et al. (2012), where they were estimated by fits to measured dark J–V curves of lattice matched 3J cells.

The temperature dependence of $E_{\mathrm{gap},i}(T)$ is implemented according to Varshni (1967):

$$E_{\mathrm{gap},i}(T) = \frac{E_{i0} - \propto_i T^2}{T + \beta_i} \tag{5}$$

Here, the parameters $E_{i0}, \propto_i$ and β_i for the $Ga_{0.50}In_{0.50}P$, $Ga_{0.99}In_{0.01}As$ and Ge sub cells were taken from Levinshtein et al. (1996, 1999).

The series resistances of the solar cells are considered in the model as one lumped resistance with $R_S = 20\ \mathrm{m\Omega\,cm^2}$. This means that the series interconnections between the sub cells are assumed to be ideal, without the presence of tunnel diodes. Normally, the parallel resistance for commercial solar cells is very high and thus is assumed to be $R_P = \infty$. In our simulation, every series connected solar cell

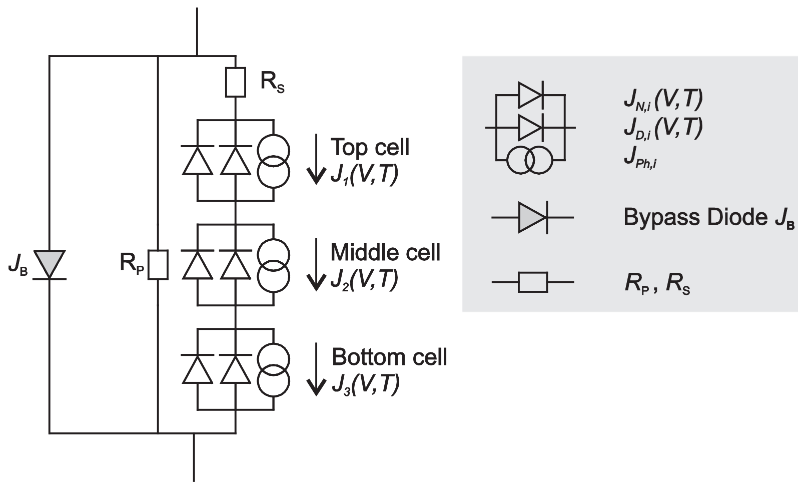

Fig. 1. Electrical structure of a 3J solar cell. The three sub cells are simulated using the two diode model with a lumped series resistance R_S and a shunt resistor R_P in parallel. The figure also shows the usage of a bypass diode with current density J_B, which is implemented in the simulation using the one diode model.

is connected with a bypass diode in parallel, since this is often the case for CPV modules. The current density of the bypass diodes $J_B(V,T)$ is expressed by the one diode model

$$J_B(V,T) = J_{0,\mathrm{Bypass}}(T)\left[\exp\left[-\frac{qV}{n_1 k_B T}\right] - 1\right], \quad (6)$$

with $n_1 = 1.0045$ and a fit function for $J_{0,\mathrm{Bypass}}(T)$. The latter is derived out of measured dark I–V curve data (see Fig. 2). It is assumed that the parallel resistance for the bypass diode is $R_P = \infty$.

2.1.2. Simulation of a CPV module

For the subsequent performed case study, three CPV modules with different interconnection schemes, shown in Fig. 3, are simulated. The *serial module* consists of 72 series connected 3J solar cells. Each of them is connected with a bypass diode in parallel. The *mixed module* comprises of two parallel strings of 36 series connected solar cells, again connected with bypass diodes in parallel. The *parallel module* consists of 72 parallel connected solar cells. Because of the parallel interconnection of cells, no bypass diodes are included.

Cells within modules typically show slightly varying output currents. This can be explained by differences in the production quality of the cells and/or concentrator lenses. In the simulation, this can be modeled using a Gaussian

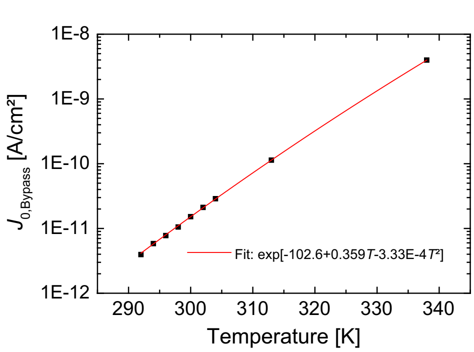

Fig. 2. Temperature dependent saturation current density of the bypass diode which was determined from a fit to measured dark I–V data.

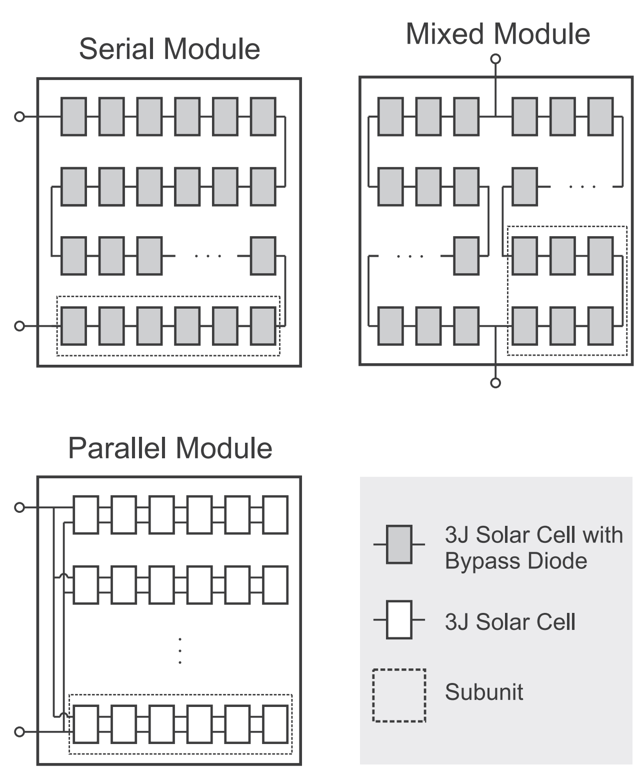

Fig. 3. Interconnection of 3J solar cells in three different module types: A *serial module* consisting of 72 series connected solar cells; a *mixed module* comprising of two parallel strings of 36 series connected solar cells; a *parallel module* consisting of 72 parallel connected solar cells. In contrast to the serial and mixed case, no bypass diodes are present at the parallel case. The dashed box indicates the choice as subunits at the procedure.

Table 1
The mean $J_{\mathrm{Ph},i}$ (one-sun) used for the simulation for the top, middle and bottom sub cell of a lattice-matched 3J cell.

Sub cell	i	Mean $J_{\mathrm{Ph},i}$ (1-sun) [mA/cm^2]
Top	1	14.6
Mid	2	14.9
Bot	3	20.8

distribution of I_{SC}'s (Antón and Sala, 2005). The mean values of the one-sun current densities used in the simulation can be found in Table 1. A standard deviation of $\sigma = 0.25$ mA/cm^2 is assumed for all three sub cells.

2.2. Stepwise measurement procedure

In this section, the stepwise measurement procedure is explained concisely. The detailed explanation can be found in Rapp et al. (2015). Here, the SMP is divided into three tasks:

(i) Segmentation of the modules into subunits,
(ii) Stepwise illumination and measurement of the modules,
(iii) Calculation of the module's illuminated I–V curve.

In the following, each of the above steps is explained and applied by means of simulation for each of the three types of CPV modules.

(i) Segmentation of the modules into subunits

The aperture area of the module is segmented into smaller subunits, which fit within the illumination area of the simulator. The actual segmentation process and the criteria that have to be fulfilled are explained in more detailed in Rapp et al. (2015). In Fig. 3, for each module type, the choice of subunits is marked with a dashed box, i.e. six single cells represent one subunit. Thus, the modules can be expressed by the selected subunits. Fig. 4 defines the nomenclature for the subsequent calculations. Notably, the *serial module* now consists of 12 series connected subunits (Case 1 with $s = 12$ and $p = 1$), the *parallel module* of 12 parallel connected subunits (Case 2 with $s = 1$ and $p = 12$) and the *mixed module* of 2 parallel strings of 6 series connected subunits (Case 1 with $s = 6$ and $p = 2$).

(ii) Simulation of the stepwise illumination and measurement of the modules

For every module type, the simulation follows the same steps: The module's I–V curve is simulated whereby the first subunit is illuminated while all others are shaded. The I–V curve obtained from this simulation is referred to as the partially illuminated (PI) I–V curve of the first subunit $I^{\mathrm{PI}[1,1]}$. The partially illuminated I–V curves of all subunits $I^{\mathrm{PI}[k,l]}$ with $k \in \{1,\ldots,s\}$ and $l \in \{1,\ldots,p\}$ are successively simulated. Additionally, the dark I–V curve of the full module I^{D} is simulated. Fig. 5 shows the 12 simulated partially illuminated (solid lines) and the simulated dark I–V curve (solid line, marked with squares) for the serial, parallel and mixed module types.

(iii) Calculation of the modules' illuminated I–V curves

The derivations of the formulas for the two cases illustrated in Fig. 4 are presented in Rapp et al. (2015, p. 4-5). For the cases of series and mixed interconnection schemes, the formula to calculate the illuminated I–V curve is

$$I^{\mathrm{I}}(V) = \sum_{l}^{p}\left[\left[\sum_{k}^{s}\left[I^{\mathrm{PI}[k,l]} - \frac{p-1}{p}\cdot I^{\mathrm{D}}\right]^{-1}\right] - (s-1)\cdot\left[\frac{I^{\mathrm{D}}}{p}\right]^{-1}\right]^{-1}, \quad (7)$$

for the parallel module

$$I^{\mathrm{I}}(V) = \left[\sum_{k}^{s}\left[\left[\sum_{l}^{p}\left[V^{\mathrm{PI}[k,l]} - \frac{s-1}{s}\cdot V^{\mathrm{D}}\right]^{-1}\right] - (p-1)\cdot\left[\frac{V^{\mathrm{D}}}{s}\right]^{-1}\right]^{-1}\right]^{-1}. \quad (8)$$

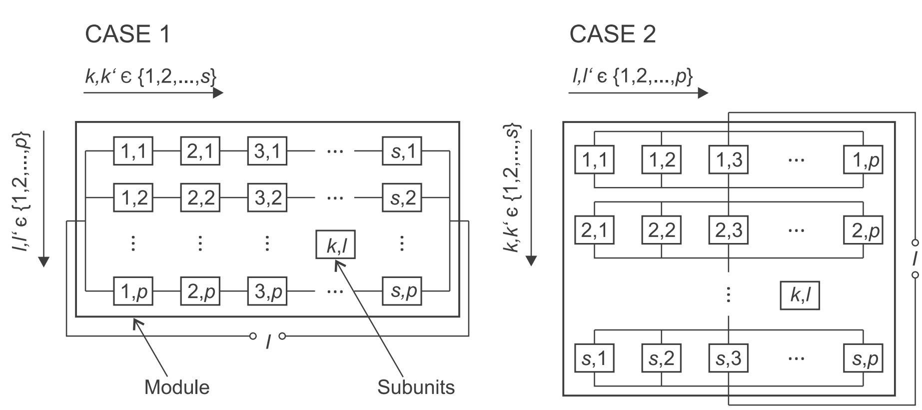

Fig. 4. A general module type with p parallel and s series connected subunits. Every subunit is clearly identified by the two indices k and l:k denotes the location of the subunit in the serial string(s); l denotes the location of the subunit in the parallel string(s). The total number of subunits is $n = s \cdot p$.

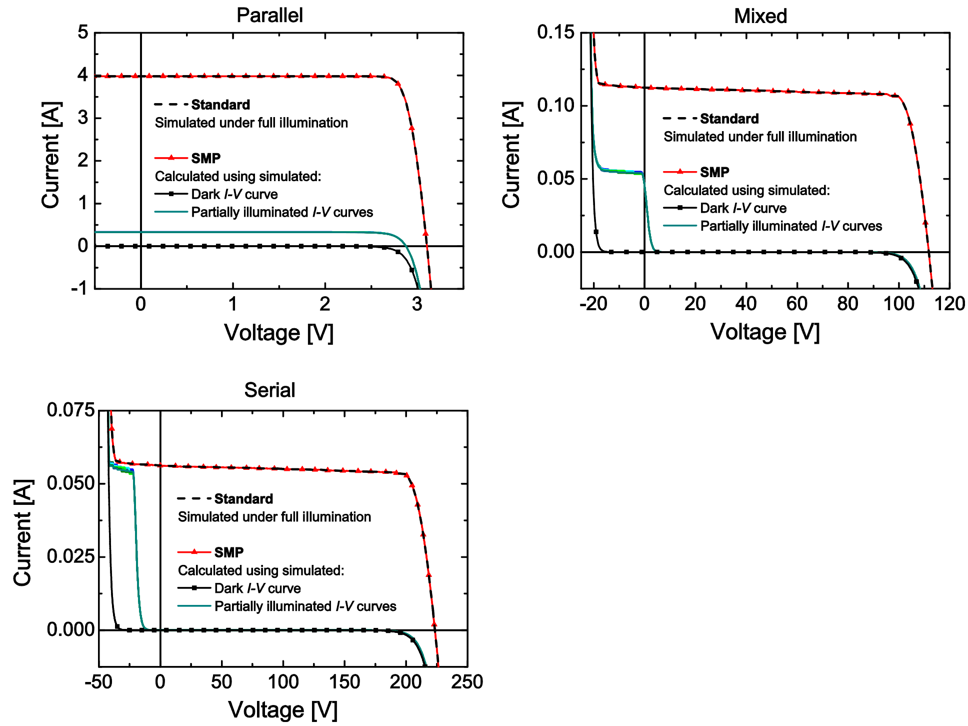

Fig. 5. The simulated partially illuminated (solid lines) and dark I–V curves (solid lines, marked with squares) for a module consisting of parallel interconnected subunits, series interconnected and one with mixed interconnections. Using the simulated dark and partially illuminated I–V curves, the I–V curve of the illuminated module (solid line, marked with triangles) is calculated and can be compared with the simulated "standard" I–V curve (dashed line), when the module is fully illuminated.

Here, the superscript (-1) denotes an inversion with which a function $f: A \to B$ can be converted to $f^{-1}: B \to A$. It has to be noted that in the derivation of both equations it was assumed that every string of subunits has the same dark I–V curve.

For each of the three cases, the equations can be adapted by choosing s and p as defined in the segmentation process. Fig. 5 shows the calculated I–V curves of the SMP (solid lines, marked with triangles) for the three module types. These can be compared with the simulations of the fully illuminated module (dashed lines), which will hereinafter be referred to as the "standard" curve.

3. Influence of measurement conditions on the accuracy of the SMP

In a realistic application environment, conditions like temperature, stray light and cell characteristics within the modules might change. In the following sections, the influence of these factors on the accuracy of the SMP is investigated.

3.1. Influence of temperature variation during the SMP

For the SMP, n partially illuminated and one dark I–V curve have to be measured. During the measurement process, a small change in room temperature and thus of the module can occur. Since the temperature is always different over time, an emphasis is placed on the case where the biggest influence on the accuracy is expected. Performing some mathematical steps on Eqs. (7) and (8), it can be found that the extreme case is present when all partially illuminated I–V curves $I^{\mathrm{PI}[k,l]}$ are measured at one temperature level and the dark I–V curve I^{D} at a deviating level. In the following, the effect of this temperature change on the calculated I–V curve of the module using the SMP is researched.

Fig. 6 shows the temperature dependent simulation results for the three different interconnected modules. The solid curves indicate the calculated I–V curves using the SMP. ΔT denotes the temperature change between the simulation of the partially illuminated I–V curves (always simulated at 25 °C) and the dark I–V curves (simulated at $25\,°\mathrm{C} + \Delta T$), which were used for the calculation. The dashed line shows the "standard" simulation of the fully illuminated module at 25 °C.

3.1.1. Parallel interconnection

In Fig. 6, the top left I–V curves show the case of a module consisting of parallel interconnected subunits. Simulating a rising temperature $\Delta T > 0\,\mathrm{K}$ between the partially illuminated (25 °C) and the dark I–V curves (>25 °C), the calculated I–V curves using the SMP shift to larger voltages. This can be explained by a dropping knee voltage (when the diode starts to conduct) and thus by a larger negative current of the dark I–V curve for rising temperatures. Adapting Eq. (8) for the present case ($p = 12$ and $s = 1$)

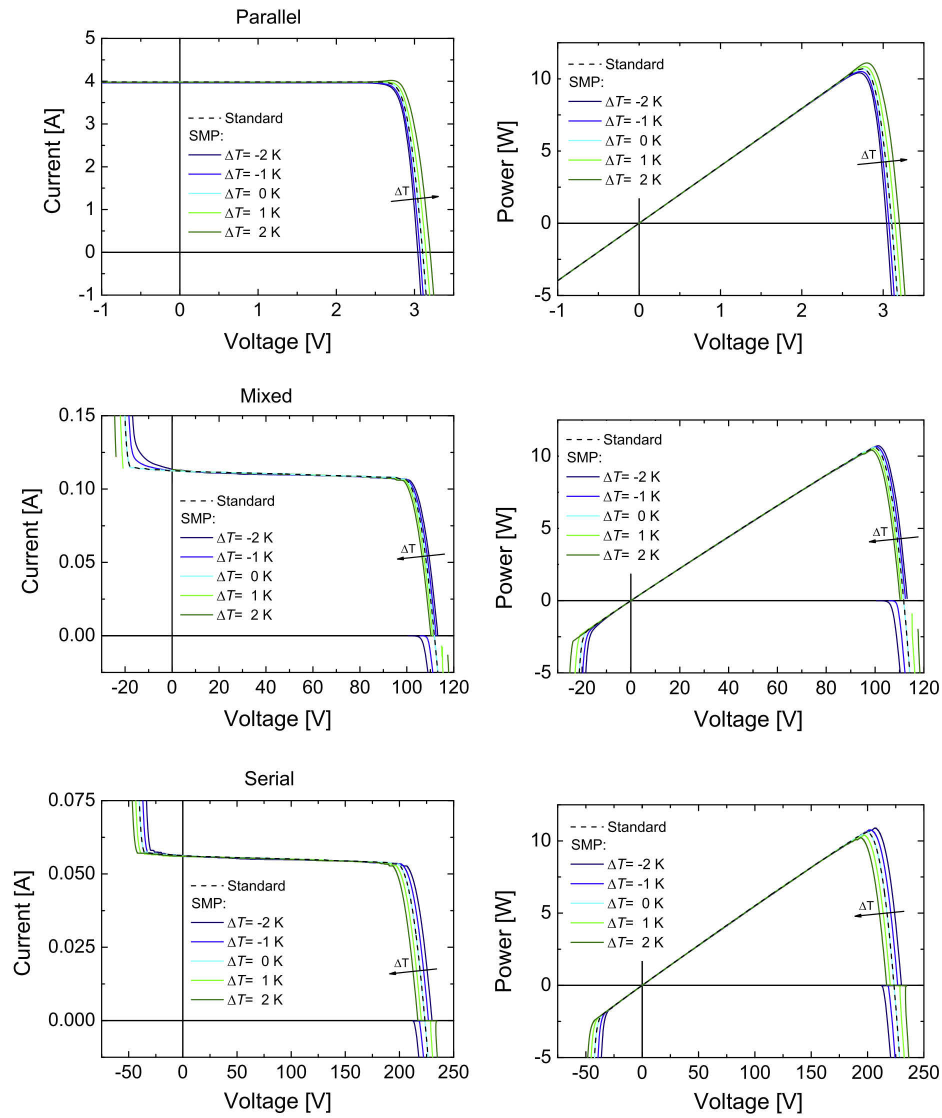

Fig. 6. The effect of a changing temperature during the SMP is investigated. The solid lines show the results of the SMP for different temperature changes (during the procedure). They can be compared with the "standard" simulation at 25 °C. A rising temperature between the measurement of the partially illuminated and dark *I–V* curves leads to a shift of the calculated *I–V* curves to larger voltages (parallel case), to singularities (serial and mixed case) and even to undefined domains (mixed case). The same behavior can also be observed in the *P–V* curves at the right column.

$$I^{\mathrm{I}}(V) = \sum_{l}^{12} I^{\mathrm{PI}[1,l]} - 11 \cdot I^{\mathrm{D}}, \tag{9}$$

one can see that the subtraction of a larger negative I^{D} leads to a larger $I^{\mathrm{I}}(V)$. This effect can also be observed in the *P–V* characteristics (Fig. 6, top right). Thus, this temperature effect leads to an error of $\Delta V_{\mathrm{OC}}/\Delta T = 1.3\%/\mathrm{K}$ and $\Delta P_{\mathrm{MPP}}/\Delta T = 1.6\%/\mathrm{K}$, whereas the I_{SC} is not affected.

3.1.2. Serial interconnection

For a module consisting of only series connected solar cells, the simulation at a stable temperature of 25 °C shows the same results between the SMP and the "standard" simulation (Fig. 6, bottom left). Simulating an increasing temperature difference between the partially illuminated *I–V* curves and the dark *I–V* curves, a singularity around the V_{OC} of the calculated *I–V* curves arises: the *I–V* curves above $I = 0$ A are shifted to a smaller voltage and the curves below $I = 0$ A are shifted to larger voltages. To explain this effect, Eq. (7) is adapted for the serial case ($s = 12$ and $p = 1$) and written as a voltage function

$$V^{\mathrm{I}}(I) = \sum_{k}^{12} \left[I^{\mathrm{PI}[k,1]}\right]^{-1} - 11 \cdot \left[I^{\mathrm{D}}\right]^{-1}. \tag{10}$$

Above $I = 0$ A, the higher temperatures lead to a smaller negative knee voltage of I^{D} (respectively the bypass diodes) and thus to a smaller voltage $V^{\mathrm{I}}(I)$. Below $I = 0$ A, the higher temperatures lead to a smaller positive knee voltage of I^{D} and thus to a larger Voltage $V^{\mathrm{I}}(I)$.

Again, these effects can also be observed in the *P–V* characteristics. Thus, a changing temperature leads to an error of $\Delta V_{OC}/\Delta T = 1.4\%/\mathrm{K}$ and $\Delta P_{MPP}/\Delta T = 1.8\%/\mathrm{K}$, whereas the I_{SC} is hardly affected.

3.1.3. Mixed interconnection

As this module comprises of parallel and series interconnections, the effects of both interconnection types can be observed in Fig. 6, middle. Above $I = 0$ A the temperature impact of both interconnection types are opposite, for which the effect for the mixed interconnection is smaller. For PV in general, the region of negative voltage and negative current of the *I–V* curve are normally not of great interest. For the sake of completeness, it is noted that the undefined domains at negative voltages and negative currents can be explained by non-monotonous *I–V* curves. These occur during the summation of the two parallel strings in Eq. (7). In these domains, no *I–V* curve can be calculated. Here, one possibility is to divide the non-monotonous curves into monotonous sections where the *I–V* curve can be calculated. If this is not possible, undefined domains will occur. At this mixed interconnection, the changing temperature leads to an error of $\Delta V_{OC}/\Delta T = -0.66\%/\mathrm{K}$ for $I > 0$ A and $\Delta P_{MPP}/T = -0.7\%/\mathrm{K}$, whereas the I_{SC} is hardly affected.

3.1.4. Conclusion

This investigation shows that a temperature change during the measurement of the various *I–V* curves which are needed for the SMP could lead to significant deviations in the calculated *I–V* curves. The biggest impact can be found near the V_{OC}. The P_{MPP} is less and the I_{SC} mostly unaffected. The maximum error for the P_{MPP} corresponds to a module with series interconnections, and is determined to be $\Delta P_{MPP}/\Delta T = 1.8\%/\mathrm{K}$. Thus, an important factor for the practical application of the procedure is to keep the temperature stability better than 1 K. However, it has to be noted that the extreme case was investigated, which means that the impact for real temperature profiles will always be lower.

3.2. Influence of stray light

The influence of stray light on the accuracy of the SMP is investigated. Therefore we distinguish between two types of stray light. The main characteristic of the first type is that at each partially illumination, its influence on the solar cells of the shaded subunits is constant. On the contrary to that, the intensity and location (within the module) of the second type of stray light changes at each partially illumination.

The first type will be called *constant stray light*. Possible origins of constant stray light are sketched in Fig. 7. Here, imperfect shading (respectively partly transparent) coverages (c) or – e.g. for modules with a glass frame – light, that leaks sideways into the module (d) lead to a illumination of the shaded solar cells. Irrelevant which subunit is illuminated, the intensity and location of this type of stray light, is assumed to stay the same at each illumination step during the stepwise illumination process.

The second type will be called *varying light*. Like illustrated in Fig. 7(b), this can be caused by for example, a misalignment and inaccuracies of the aperture which detaches the illuminated subunit from the surrounding shaded subunits. Thus cells which are in the neighborhood of the illuminated subunit might get illuminated during the measurement of the partially illuminated *IV* curves. Main characteristic of this type of light is, that its location within the module changes for each step of the partially illumination process.

3.2.1. Constant stray light

For the simulation of the partially illuminated *I–V* curves, stray light of $c_{stray} = 1\%$ (which corresponds to very poorly shading coverages) is assumed to leak constantly into all shaded subunits (Figs. 7(c) and 8, left). For the calculation of the illuminated *I–V* curve, two cases concerning the dark *I–V* curve are now investigated: In case (i) the dark *I–V* curve

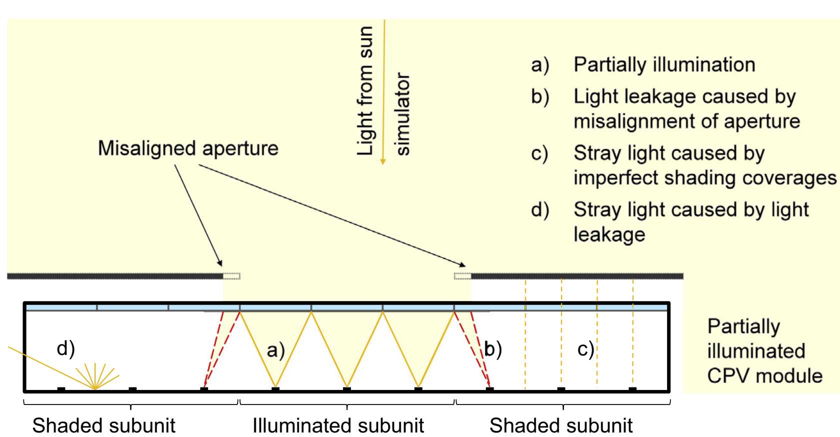

Fig. 7. Illustration of constant and varying light, which can occur when a CPV module is partially illuminated. A subunit (a) is illuminated, while all other subunits are shaded. Misaligned apertures can lead to a light leakage onto neighboring cells of shaded subunits (b). At the illumination of different subunits, different cells get affected by this varying light. Constant stray light can for example be caused by imperfect shading (partially-transparent) coverages (c) and light leakages (d). For each partially illumination (of different subunits), the influence on the shaded cells is assumed to be constant.

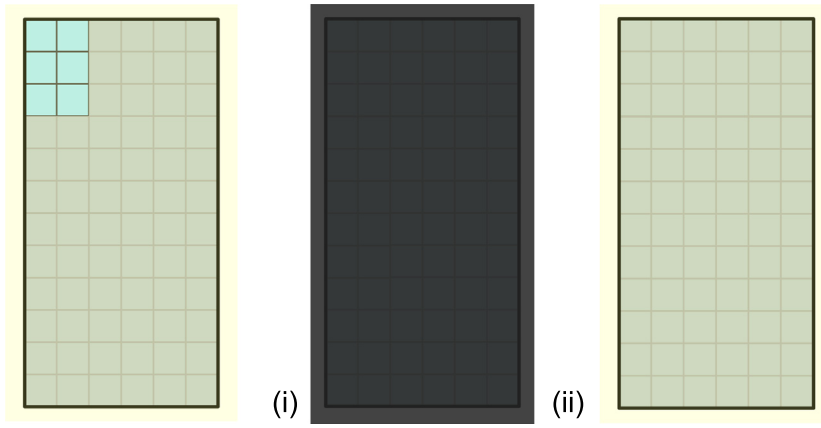

Fig. 8. To exemplify the influence of constant stray light, an illuminated module with covered subunits is shown. Left: Because of e.g. non-perfect coverages, light might leak into the shaded subunits during the partial illumination. For the measurement of the dark I–V curve, two ways are conceivable: (i) the module is perfectly shaded (true darkness), or like shown in (ii), the module is exposed to the same stray light influence compared to the shaded subunits at the partially illumination (left). In the last case the module is covered by the shading and also illuminated by the sun simulator.

of the *perfectly shaded* module (Fig. 8(i)) is used to calculate the illuminated I–V curve. In (ii) as "dark" I–V curve, an I–V curve with the same *stray light influence* as occurred in the (shaded areas) at the partially illumination (Fig. 8(ii)) is used. That means, the same shading as at the partially illumination covers the whole module, which is then illuminated by the sun simulator. This I–V curve will be called "dark" I–V curve with stray light influence.

Fig. 9 shows the simulated I–V curves of the three different module types using the SMP (solid lines) and the "standard" method which is simulated without any stray light influence (dashed). The SMP is calculated firstly using (i) the perfectly shaded dark I–V curve, and secondly using (ii) a "dark" I–V curve which is influenced by the constant stray light.

3.2.1.1. Parallel Interconnection.

(i) For the module with parallel interconnection, the calculation of the illuminated I–V curve using the SMP with a perfectly shaded dark I–V curve shows a much higher current compared to the "standard" procedure (see Fig. 9, top left). With reference to Eq. (8) and including stray light, it can be determined that the I^*_{SC} using the perfectly dark I–V curve for the SMP is: $I^*_{SC} = I_{SC} + (p-1)\cdot 0.01 \cdot I_{SC}$. Therefore, the stray light into the $(p-1)$ subunits leads to an error of $\Delta I_{SC} = (p-1)\cdot c_{stray}$ and thus to an error in the maximum power point of approximately $\Delta P_{MPP} \approx (p-1)\cdot c_{stray}$.

(ii) If the "dark" I–V curve with stray light influence is used in the calculation (see Fig. 9, top left), the influence of the constant stray light is completely eliminated. Thus, in this case, the SMP perfectly reproduces the results of the "standard" method.

3.2.1.2. Serial and mixed interconnection.

(i) Using a perfectly shaded dark I–V curve for the calculation of the SMP, deviations to the "Standard" I–V curve around the V_{OC} can be observed (Fig. 9, middle and bottom). For the mixed case, minor deviations of around 1% between the calculated I–V curve (solid, blue) and the "standard" I–V curve (dashed, black) are also visible around the I_{SC} and P_{MPP}.

(ii) If at the SMP a "dark" I–V curve with stray light influence is used, the stray light effect gets eliminated and the I–V curve perfectly fits to the "standard" I–V curve.

3.2.2. Varying light

The previous examination demonstrates that only the parallel interconnection in combination with a fully shaded dark I–V curve shows significant deviations in the I_{SC} and P_{MPP}. The series and mixed cases, however, only show a minor influence at the maximum power point. Therefore, the impact of varying light on the parallel configuration is analyzed.

To illustrate the origin of varying light, Fig. 10 shows the illuminated section of a partially illuminated module. Here, a misaligned and inaccurate aperture leads to an illumination of adjacent Fresnel lenses and thus, like illustrated in Fig. 7, to a direct illumination of adjacent cells. The detailed impact of this adjacent light on the partially illuminated I–V curves, however, is strongly dependent on the cell interconnection within the subunits:

If the *subunits consist of parallel interconnected solar cells*, it can be approximated, that the I_{SC}s of the partially illuminated I–V curves scale with the fraction of stray light in adjacent areas $I^{PI[1,l]}_{SC,stray} = I^{PI[1,l]}_{SC}(1 + A_{adj}/A_0)$ (see Fig. 10). With regard to Eq. (9) this results in a relative overestimation of the calculated module parameters of about $\Delta I_{SC} \sim \Delta P_{MPP} \sim A_{adj}/A_0$.

If the *subunits consist of series connected solar cells*, the illumination of one neighboring cell could already strongly affect the I_{SC} of the partially illuminated I–V curve and thus, the I_{SC} of the calculated I–V curve of the module.

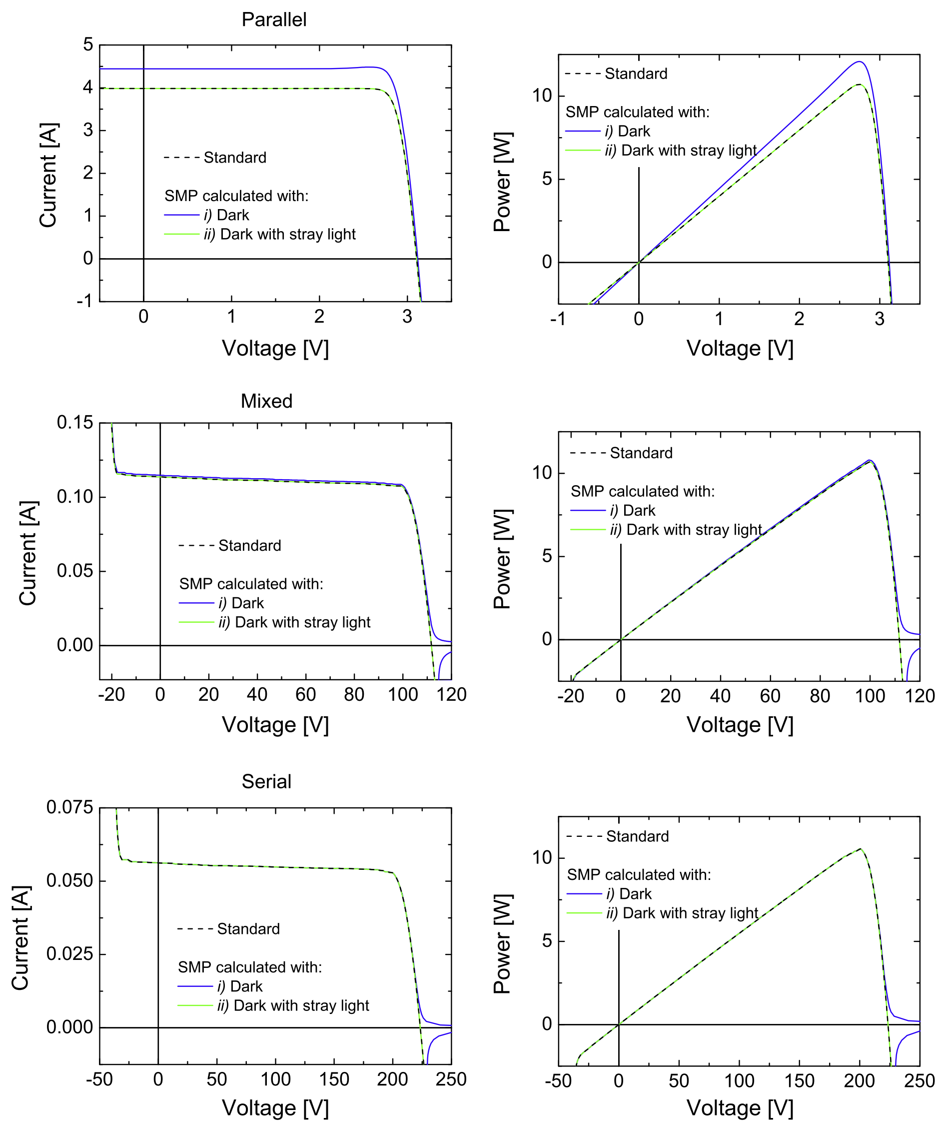

Fig. 9. The effect of constant stray light on the I–V and P–V curves using the SMP is illustrated. (i) The solid blue lines show the results of the SMP when the measurements of the partially illuminated I–V curves are affected by 1% stray light, whereas the dark I–V curve is measured *perfectly dark*. In this case strong deviations to the "standard" I–V curve can be observed. (ii) If at the calculation *a dark I–V curve with stray light influence* is used, the resulting I–V curve using the SMP (solid green) perfectly fits to the "standard" simulation (dashed black). (For interpretation of the references to color in this figure legend, the reader is referred to the web version of this article.)

The P_{MPP} however, could remain unaffected if just some cells of the neighboring subunits get illuminated.

Irrelevant which interconnection scheme is present, the upper limit of the impact on the modules power can be approximated by Eq. (A8) which is derived in Appendix A section:

$$P_{\mathrm{MPP,stray}} \leqslant P_{\mathrm{MPP}} \cdot (1 + A_{\mathrm{adj}}/A_0). \tag{A8}$$

Here, the induced deviation depends on the (mean) illuminated adjacent area A_{adj} and the Area of one subunit A_0 (see Fig. 10).

To assess the induced error, an example module with typical parameters is researched. The surface area of a subunit is assumed to be $A_0 \sim 1\ \mathrm{m}^2$ (which is ideally the size of the sun simulator's aperture). The illuminated adjacent area caused by a 0.2 cm misalignment of the aperture would be $A_{\mathrm{adj}} = 4 \cdot 100\ \mathrm{cm} \cdot 0.2\ \mathrm{cm}$. The SMP on this module (with an arbitrary subunit interconnection) would cause a maximal error in the P_{MPP} of $\Delta P_{\mathrm{MPP}} \leqslant A_{\mathrm{adj}}/A_0 = 0.8\%$. If the subunits are interconnected in parallel the maximal deviation in I_{SC} would be also $\Delta I_{\mathrm{SC}} \leqslant A_{\mathrm{adj}}/A_0 = 0.8\%$.

3.2.3. Conclusion

To investigate the influence of stray light on the result of the SMP, it was distinguished between constant stray light and varying light. The effect of constant stray light can be fully eliminated, if at the calculation a dark I–V curve with stray light influence is used. This can be explained by the fact that if the same stray light is present in the measurement of the partially illuminated I–V curves and in the

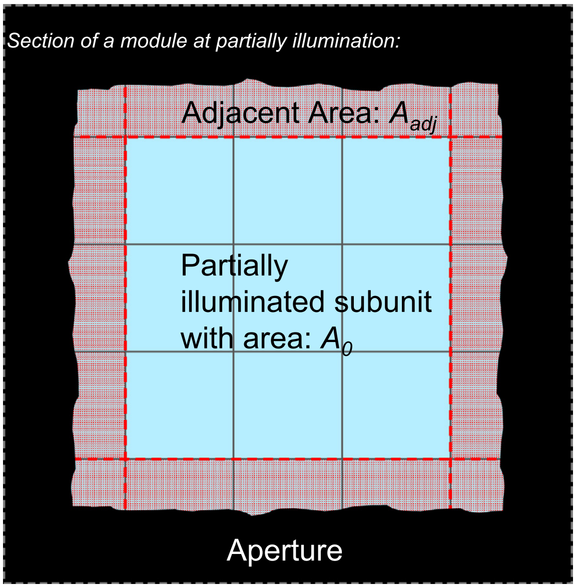

Fig. 10. The section of a partially illuminated subunit of a module is shown. The inner subunit is illuminated, while the outer subunits are shaded. Inaccuracies and misalignments of the aperture which detaches the shaded subunits from the illuminated one lead to a propagation of light in surrounding Fresnel lenses and thus into surrounding solar cells. In this example light propagates into the adjacent area of the 4 surrounding subunits with a total area of A_{adj}.

measurement of the dark I–V curve, the stray light contribution gets eliminated in the calculation. Contrary to this case, it cannot be prevented from the influence of varying light on the I_{SC} and P_{MPP} of a module with parallel interconnected subunits (the I_{SC} and P_{MPP} of a module with series subunits however stays unaffected). Here it has to be mentioned that the detailed error in I_{SC} and P_{MPP} strongly depends on the cell interconnection within the subunits. At the practical application, therefore, it is recommended to perform an error estimation for each individual case. A general estimation however illustrated, that the maximal relative error in the calculated power is $\Delta P_{MPP} \leqslant A_{adj}/A_0$. Here A_{adj} represents the area which is illuminated by adjacent light, and A_0 the surface area of one subunit. In the investigated example this lead to an error of $\Delta P_{MPP} \leqslant 0.8\%$. To minimize deviations which are induced by varying light, exact apertures and a precise alignment process has to be used.

3.3. Influence of module defects

In the derivation of Eq. (7), it was assumed that if a module consists of more than one string of subunits, each string has the same dark I–V curve (Rapp et al., 2015, p. 5, eq. 8-9). The same was assumed in the derivation of Eq. (8) (Rapp et al., 2015, p. 5, eq. 11-12). However, cells within modules can have variable cell parameters and can sometimes even have defects. This would lead to an invalidation of this assumption, and thus could result in an error in the calculated I–V curve. To research the impact of such a break of the assumption, the effects of module defects on the results of the SMP must be investigated. In this analysis, two types of defects are studied: a module which contains one cell with a high R_S and a module which contains one cell with a low R_P. For all other cells within the module, $R_P = \infty$ and $R_S = 20\,\text{m}\Omega\,\text{cm}^2$ are assumed, as in the previous cases. Fig. 11 for the R_S and Fig. 12 for the R_P investigation show the simulated I–V curves for the different resistance values using the SMP (solid) and the "standard" simulation (dashed).

3.3.1. Parallel and serial interconnection

In the parallel and series cases, for each R_S and R_P value, no deviation between the I–V curves using the SMP and the "Standard" simulation are observed, as illustrated in the top and bottom Figs. 10 and 11.

3.3.2. Mixed interconnection

In the case of mixed interconnections, minor deviations for $I > 0$ are visible (see enlarged section of Fig. 11, middle). At negative currents, which normally are not of a great interest in the characterization, also undefined domains occur. This can be explained by the fact that a module with mixed interconnections consists of more than one string of subunits. In this case, the dark I–V curve of the string which contains the "deviating" cell differs from the other one. Consequently, the assumption that the dark I–V curve of each string consists of a fraction of the module's whole dark I–V curve is no longer valid, and thus leads to slight deviations near the V_{OC} (see middle Figs. 10 and 11). The I_{SC} and P_{MPP} values however, are not affected.

3.3.3. Conclusion

This investigation shows that, in the case of a module consisting of more than one string of subunits, module defects can have an influence on the results of the SMP. These deviations are marginal and can be mainly observed near the V_{OC}, whereas the I_{SC} and P_{MPP} are not affected. To avoid this deviation, the module should be segmented into a configuration with just one string of subunits during the segmentation step. If this is not possible, another opportunity is to estimate the V_{OC} by interpolation over the undefined domain.

4. Summary and recommendations

In this paper, the impact of perturbing factors like a temperature variation (during the measurement process), stray light and module defects (high R_S and low R_P) on the results of the **S**tepwise **M**easurement **P**rocedure (SMP) was investigated. This study is based on a validated temperature dependent SPICE network model, which can simulate the I–V curves needed for the SMP. Subsequently, these dark and partially illuminated curves were used for the calculation of the I–V curves of the illuminated

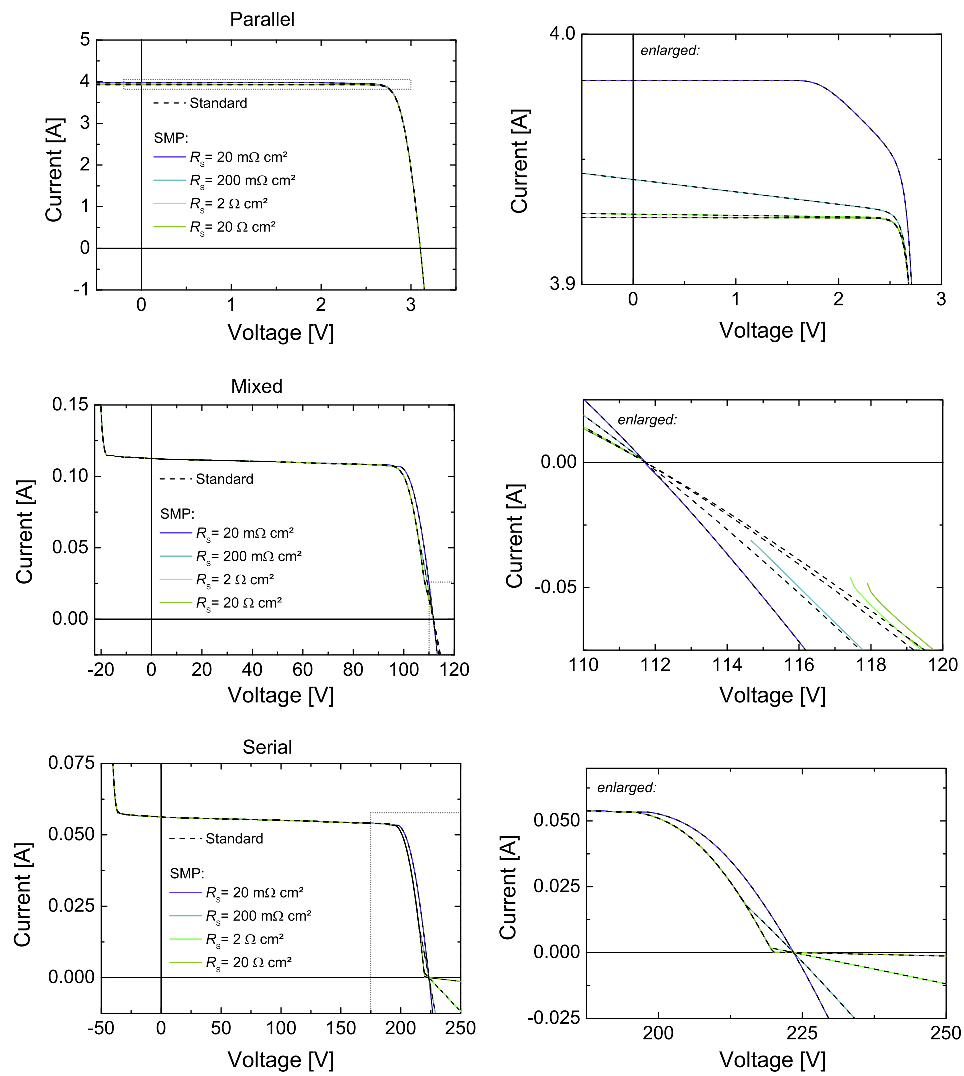

Fig. 11. The current–voltage characteristics of a module for different R_S values of one "deviating" cell are shown. The marked sections are shown enlarged at the right column. All other cells are simulated with $R_S = 20\ \text{m}\Omega\,\text{cm}^2$. The solid lines show the calculated I–V curves using the SMP for different R_S values. The dashed lines show the "standard" simulation under full illumination of the module for the same resistance values. The comparison between the SMP (solid) and the "standard" method (dashed) show no deviations for the series and parallel case, whereas for the mixed case, undefined domains and deviations around the V_{OC} can be observed (see middle, right).

modules. These results, obtained by the SMP, were compared with the "standard" simulation, which is the simulation under full illumination of the whole module. This comparison showed that a changing temperature of the test device during the measurement has an influence on the results of the SMP. Deviations were observed mainly near the V_{OC} but also close to the P_{MPP}. The maximum deviation for the P_{MPP}, which is the most interesting parameter for the SMP, is $\Delta P_{MPP}/\Delta T = 1.8\%/\text{K}$. Therefore, the temperature of a module must be kept as stable as possible during the measurements for the SMP. For the stray light investigation, we distinguished between constant stray light (which occurs at each partially illumination) and varying light (which changes at each partially illumination). It was determined that the impact of constant stray light can be eliminated. For this, as "dark" I–V curve, just an I–V curve with the same stray light influence (compared to the shaded areas at the partially illumination) has to be used at the calculation of the SMP. From the impact of varying light however cannot be prevented. This can for example be caused by aperture inaccuracies and misalignments at the shading process. A general estimation showed that the maximal error in P_{MPP} is dependent on the fraction of the area which is (because of a bad aperture) outshined A_{adj} and the surface area of one subunit A_0: $\Delta P_{MPP} \leqslant A_{adj}/A_0$. The detailed impact of this adjacent light on the I–V parameters, however, is strongly dependent on the cell interconnection within the subunits and has to be estimated in each individual case. By using exact apertures and a precise alignment, this error can be reduced further. The investigation on how module defects influence the results of the SMP showed that for modules which are segmented into just one string of either series or parallel interconnected subunits, no deviations are found. Modules

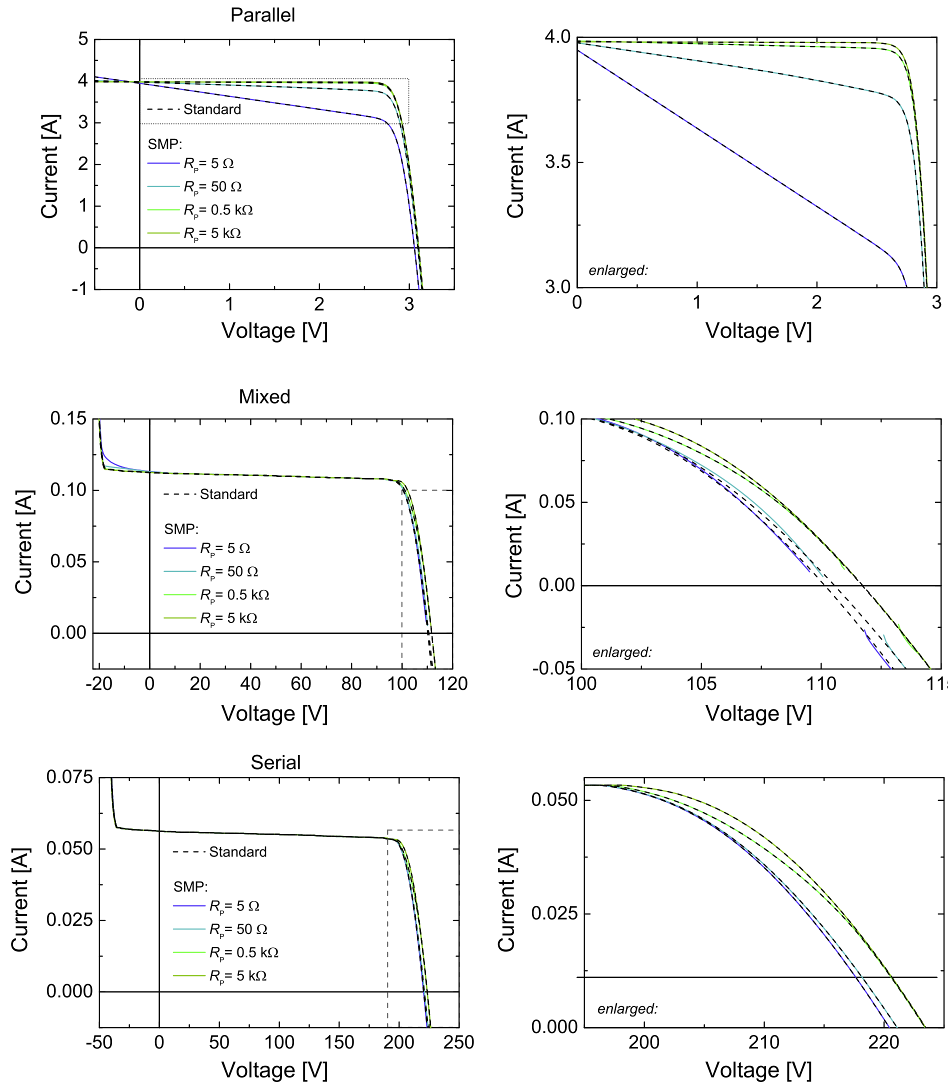

Fig. 12. The current–voltage characteristics of a module for different R_P values of one "deviating" cell are shown. The marked sections are shown enlarged at the right column. The solid lines show the calculated I–V curves using the SMP, the dashed lines using the "standard" simulation. For the series and parallel case again no deviations compared to the "standard" simulation occur. At the mixed case for rising R_P values, undefined domains and deviations around the V_{OC} arise (see middle, right).

consisting of mixed interconnections of subunits, however, can have minor deviations caused by cell variations and defects. But those mainly arise near the V_{OC}, whereas the P_{MPP} remains unaffected. To gain highest precision of the results from the procedure, the module should be segmented into just one string of subunits to avoid this effect. If this is not possible, the V_{OC} can be estimated by interpolation over the undefined domain.

Additionally to this electrical investigation it should be mentioned, that also the mechanical realization of such a solar simulator for large CPV modules can present some challenges. Here, either the module or the sun simulator itself has to be moved by a x–y stage construction. During this translation, the angle between the sun simulator and the CPV module, however, has to be as unaffected as possible. This is a prerequisite to minimize distortions caused by misalignment.

Acknowledgements

The authors would like to thank all colleagues of the "*III–V* Epitaxy and Solar Cell" group. This work has been partly supported by the Federal Ministry for Economic Affairs and Energy (BMWi) under the CPVMagnus project, contract number 0325485D, and by the European Commission under the project NGCPV with Grant agreement no. 283798. The authors are responsible for the content of this work.

Appendix A

The influence of varying light on a module with a parallel subunit interconnection is investigated. At each partially illumination step l, the measured I–V curve $I^{PI[1,l]}$ gets overestimated by the influence of varying stray light (see Fig. 10). The detailed impact on the maximum power point $P^{PI[1,l]}_{MPP,stray}$ (of each partially illuminated I–V curve with varying stray light), however, is just determinable, if the I–V curves of the i adjacent subunits with stray light I_i^{stray} (with $i \in \{1, \ldots, s \cdot p\} \setminus l$) are known:

$$P^{PI[1,l]}_{MPP,stray} = \max\left(I^{PI[1,l]}_{stray} \cdot V\right) = \max\left(I^{PI[1,l]} \cdot V + I_1^{stray} \cdot V + I_2^{stray} \cdot V + \ldots\right). \tag{A1}$$

The upper limit of this term, however, can be estimated by writing:

$$P^{PI[1,l]}_{MPP,stray} \leqslant \max(I^{PI[1,l]} \cdot V) + \underbrace{\max\left(I_1^{stray} \cdot V\right)}_{P_1} + \underbrace{\max\left(I_2^{stray} \cdot V\right)}_{P_2} + \ldots \tag{A2}$$

Assuming that the power of all surrounding subunits $P_1, P_2, \ldots$ can be expressed by the power of the partially illuminated subunit $P^{PI[1,l]}_{MPP}$ in combination with a scaling factor which just depends on the fraction of the illuminated adjacent area $A_{adj,i,l}$ of each subunit i compared to the total area A_0 of a subunit, Eq. (A2) turns to:

$$P^{PI[1,l]}_{MPP,stray} \leqslant P^{PI[1,l]}_{MPP} + P^{PI[1,l]}_{MPP} \cdot A_{adj,1,l}/A_0 + P^{PI[1,l]}_{MPP} \cdot A_{adj,2,l}/A_0 + \cdots \tag{A3}$$

Using the total adjacent area which is affected by the stray light $A_{adj,l} = A_{adj,1,l} + A_{adj,2,l} + \cdots$, the P_{MPP} of the l-th partially illuminated I–V curve can be written as:

$$P^{PI[1,l]}_{MPP,stray} \leqslant P^{PI[1,l]}_{MPP} \cdot \left(1 + \frac{A_{adj,l}}{A_0}\right). \tag{A4}$$

Now, Eq. (9) which describes the I–V curve of a parallel module, can be modified by multiplying with V_{MPP} to an equation of the Power:

$$P_{MPP,stray} = \sum_l^{12} P^{PI[1,l]}_{MPP,stray} - 11 \cdot P^D. \tag{A5}$$

Inserting Eq. (A4) we get:

$$P_{MPP,stray} \leqslant \underbrace{\sum\nolimits_l^{12} P^{PI[1,l]}_{MPP} - 11 \cdot P^D}_{P_{MPP}} + \sum_l^{12} P^{PI[1,l]}_{MPP} \cdot A_{adj,l}/A_0. \tag{A6}$$

Assuming, that at each partially illumination l the same area $A_{adj,l} = A_{adj}$ gets outshined, we get:

$$P_{MPP,stray} \leqslant P_{MPP} + A_{adj}/A_0 \sum_l^{12} P^{PI[1,l]}_{MPP}. \tag{A7}$$

Now, the right side of this term is enlarged by adding $11 \cdot |P^D| \cdot A_{adj}/A_0$. As the power of the dark I–V curve is negative: $\mathrm{sgn}(P^D) = -1$, Eq. (A7) turns to

$$P_{MPP,stray} \leqslant P_{MPP} + A_{adj}/A_0 \underbrace{\left(\sum\nolimits_l^{12} P^{PI[1,l]}_{MPP} - 11 \cdot P^D \cdot\right)}_{P_{MPP}}. \tag{A8}$$

This shows, that in a worst case scenario, varying light leads to a relative overestimation of the P_{MPP} of

$$\Delta P_{MPP} \leqslant A_{adj}/A_0, \tag{A9}$$

which is just dependent on the fraction of the area which is affected by varying light A_{adj} compared to the total area of one subunit A_0.

References

Antón, I., Sala, G., 2005. Losses caused by dispersion of optical parameters and misalignments in PV concentrators. Prog. Photovolt.: Res. Appl. 13, 341–352.

Levinshtein, M., Rumyantsev, S., Shur, M., 1996. In: Si, Ge, C (Diamond), GaAs, GaP, GaSb, InAs, InP, InSb, Handbook Series on Semiconductor Parameters, vol. 218. World Scientific Publishing, Singapore.

Levinshtein, M., Rumyantsev, S., Shur, M., 1999. Ternary and quaternary III–V compounds. In: Handbook Series on Semiconductor Parameters. World Scientific Publishing, Singapore, p. 205.

Lv, H., Sheng, F., Dai, J., Liu, W., Cheng, C., Zhang, J., 2015. Temperature-dependent model of concentrator photovoltaic modules combining optical elements and III–V multi-junction solar cells. Sol. Energy 112, 351–360.

Mathiak, G., Bork, A., Schäfer, C., Bous, F., Rimmelspacher, L., Herrmann, W., 2014. Further development of a pulsed solar simulator for CPV modules and acceptance angle measurement. In: Proceedings of the EU PVSEC, 29th, pp. 2072–2075.

Ota, Y., Nishioka, K., 2012. Three-dimensional simulating of concentrator photovoltaic modules using ray trace and equivalent circuit simulators. Sol. Energy 86, 476–481.

Plesniak, A., Garboushian, V., 2011. A profile of the Amonix 7700 CPV solar power system. Proc. High Low Concent. Syst. Solar Electr. Appl. VI, 810803–810807.

Rapp, C., Steiner, M., Siefer, G., Bett, A.W., 2015. Stepwise measurement procedure for the characterization of large-area photovoltaic modules. Prog. Photovolt.: Res. Appl. 23, 1867–1876.

Reinhardt, K.C., Yeo, Y.K., Hengehold, R.L., 1995. Junction characteristics of $Ga_{0.5}In_{0.5}P$ n+p diodes and solar cells. J. Appl. Phys. 77, 5763–5772.

Steiner, M., Philipps, S.P., Hermle, M., Bett, A.W., Dimroth, F., 2010. Validated front contact grid simulation for GaAs solar cells under concentrated sunlight. Prog. Photovolt.: Res. Appl. 19, 73–83.

Steiner, M., Guter, W., Peharz, G., Philipps, S.P., Dimroth, F., Bett, A. W., 2011. A validated SPICE network simulation study on improving tunnel diodes by introducing lateral conduction layers. Prog. Photovolt.: Res. Appl. 20, 274–283.

Steiner, M., Siefer, G., Bett, A.W., 2012. An investigation of solar cell interconnection schemes within CPV modules using a validated temperature-dependent SPICE network model. Prog. Photovolt.: Res. Appl. 22, 505–514.

Varshni, Y.P., 1967. Temperature dependence of the energy gap in semiconductors. Physica 34, 149–154.